Generation of mouse models of lymphoid neoplasm using retroviral gene transduction of *in vitro*-induced germinal center B and T cells

Kotaro ARITA, M.D.

Department of Gastroenterology and Hematology

Graduate School of Medicine and Pharmaceutical Science for Education

Generation of mouse models of lymphoid neoplasm using retroviral gene transduction of *in vitro*-induced germinal center B and T cells.

Kotaro Arita[1,2] Yumiko Maeda-Kasugai[1], Koichi Ohshima[3], Shinobu Tsuzuki[1], Miyuki Suguro-Katayama[1], Kennosuke Karube[1], Noriaki Yoshida[1,4], Toshiro Sugiyama[2], and Masao Seto[1, 4]

[1] Division of Molecular Medicine, Aichi Cancer Center Research Institute 1-1, Kanokoden, Chikusa-ku, Nagoya, Aichi, 464-8681, Japan
[2] Third Department of Internal Medicine, Graduate School of Medicine and Pharmaceutical Sciences, University of Toyama, 2630 Sugitani, Toyama, Toyama, 930-0152, Japan
[3] Department of Pathology, School of Medicine, Kurume University, 67 Asahi-machi, Kurume, Fukuoka, 830-0011, Japan
[4] Department of Cancer Genetics, Program in Function Construction Medicine, Nagoya University Graduate School of Medicine, 65 Tsurumai-cho, Nagoya, Aichi, 466-8550, Japan

Corresponding author: Shinobu Tsuzuki M.D., Ph.D., Division of Molecular Medicine, Aichi Cancer Center Research Institute, 1-1 Kanokoden, Chikusa-ku, Nagoya, 464-8681, Japan, phone: +81-52-762-6111, fax: +81-52-763-5233, email: stsuzuki@aichi-cc.jp

Running title: *In vitro* B and T cell gene transduction system for lymphoma research

The authors declare no competing financial interests.

New Techniques and Technologies/Malignant hematopoiesis
Word count: 3512

Abstract

Evidence is accumulating that hematological malignancies develop following acquisition of multiple genetic changes. Despite providing many insights into the way by which given genetic changes contribute to the development of disease, the generation of animal models is often laborious. Here we show a simplified method that allows the retroviral transduction of genes of interest into mouse B or T cells, thus leading to the rapid generation of models of lymphoid neoplasm in mice. Specifically, germinal center B cells induced *in vitro* from naïve mouse B cells and infected with retroviruses for *Myc* and *Bcl2* rapidly developed a neoplasm of immunoglobulin-expressing mature B cells in transplanted mice. Likewise, T cells induced *in vitro* from immature hematopoietic cells and infected with retroviruses for *Myc*, *Bcl2* and *Ccnd1* rapidly developed CD4+CD8- and CD4+CD8+ T cell neoplasm in transplanted mice. These findings support the utility of our simplified method as a versatile tool for lymphoma research.

Introduction

Evidence is accumulating to suggest that lymphomas develop as a result of the acquisition of multiple genetic changes. Although *Myc* is a potent oncogene, transgenic expression of Myc alone in the lymphoid compartment of hematopoietic cells in mice appears insufficient to elicit the development of lymphoma, as myc-expressing pre-B cells expand as a benign state in Eμ-Myc transgenic mice [1][2]. Subsequent experiments employing compound mice generated by crossing transgenic mice have unequivocally shown that Myc collaborates with genes such as Bcl2 [3], Ccnd1 [4] and Bmi1 [5] to induce lymphoma in mice. Although these experiments are valuable, the generation and crossing of genetically engineered mice to facilitate multiple gene expression is laborious, thus making it difficult to study the roles of

combinations of multiple genes in the development of lymphomas. In this respect, use of a mouse transplantation model employing retroviral gene transduction into hematopoietic cells is feasible in many cases. However, this type of approach has been hampered by a lack of established methods that allow efficient gene transduction into normal counterparts of cells in which lymphomas originate, such as germinal center B (GCB) cells. In the study presented here, we induced GCB cells *in vitro*, facilitated the expression of multiple genes of interest through retroviral transduction, and then transplanted the gene-transduced cells into mice. Given that “double-hit” lymphomas involving deregulated expression of Myc and Bcl2 [6] represent a clinically dismal disease, we chose to model the lymphoma by employing our methodology in order to demonstrate the utility of our system for lymphoma research. In a similar initiative, we utilized T cells induced from hematopoietic progenitor cells for retroviral gene transduction and subsequent generation of mouse models of T cell neoplasms.

Materials and methods

Induction of GCB cells *in vitro*, retroviral infection, and transplantation

Induction of GCB cells was performed essentially as described in the literature [7]. Briefly, B220+ B cells isolated from the spleens of C57BL/6 mice were co-cultured with X-ray(150-Gy)-irradiated NIH3T3 cells engineered to express mouse CD40 ligand and mouse Baff (3T3/CD40L/Baff cells), in the presence of mouse IL4 (1 ng/ml; PeproTech) for 4 days. B cells were subsequently transferred onto a new layer of 3T3/CD40L/Baff cells, and cultured in the presence of mouse IL21 (10 ng/ml; PeproTech) for 2 days. 3T3/CD40L/Baff cells were generated by infecting NIH3T3 cells with retroviruses for mouse Baff (MSCV-mouse *Baff*/pgk-puro^{R}) and mouse CD40L (MSCV-mouse *CD40l*/pgk-blasticidin^{R}),

and selected for drug resistance with puromycin and blasticidin (Sigma). cDNA for mouse *Baff* was obtained by the PCR method using cDNA from mouse bone marrow and spleen cells, and cDNA for mouse *CD40L* was generously provided by Dr. T. Tsubata (Tokyo Medical and Dental University). Retrovirus was produced as described [8] and infected into cells on the 5th and 6th days after initiation of the culture. Cells were subsequently harvested by vigorous pipetting, filtered through 42-μm and 15-μm nylon meshes, and transplanted (5-10 × 10^6 cells) intraperitoneally into NSG mice (NOD.Cg-*Prkdc*^{scid}*Il2rg*^{tm1Wjl}/SzJ: purchased from the Jackson Laboratory), or intravenously into sublethally irradiated (5 Gy) syngeneic hosts.

Induction of T cells *in vitro*, retroviral infection, and transplantation

Fetal liver cells isolated from 14 d.p.c. Balb/c mice (Charles River) were depleted of Ter119-positive cells and co-cultured with an X-ray(15-Gy)-irradiated OP9-Dl1 stromal cell (RIKEN BRC) layer in the presence of mouse Flt3 (FMS-like tyrosine kinase 3) ligand (5 ng/mL; PeproTech) and 0.5–1.0% of culture supernatant of the mouse IL-7-producing cell line J558L-IL7 (kindly provided by Dr. A. G. Rolink, University of Basel), as described [9]. Cells were harvested and seeded at 5×10^4 cells/well onto a fresh OP9-Dl1 layer every 7 days. Cells were infected with retrovirus on day15 after initiation of culture, and transplanted (7–10×10^6) intravenously into lethally irradiated syngeneic hosts together with 1x10^6 fresh bone marrow cells for radioprotection. Cells obtained from spleen were used for secondary and tertiary transplantations. Purified CD4+ cells were used in some transplantation experiments. All animal experiments were performed according to protocols approved by the Institutional Animal Care and Use Committee at the Aichi Cancer Center.

Retroviral plasmids

Retroviral vectors for Myc (MSCV-*Myc*-ires-*GFP*), Bcl2 (MSCV-*Bcl2*-ires-human (h) *CD8*), and Myc plus Bcl2 (MSCV-*Bcl2*-pgk-*Myc*-ires-*GFP)* were constructed as described [8]. MSCV-*Ccnd1-human (h) CD4* was constructed by inserting cDNA for mouse *Ccnd1* into the EcoRI restriction site of the MSCV-ires-*hCD4* vector (a generous gift by Dr. J.G. Cyster, UCSD). CSII-EF1-ires2-Venus lentiviral vector was obtained from RIKEN BRC with the permission of Drs. H. Miyoshi and A. Miyawaki (RIKEN), and transfected together with pCAG-HIVg/p and pCMV-VSVG/RSV-Rev plasmids (RIKEN BRC) into 293T cells to produce virus [10].

Flow cytometry

Antibodies for mouse B220(RA3-6B2), IgD(11.26c), IgG1(X-56; MiltenyiBiotec), GL7(GL7), Fas(15A7), B7-1/CD80(16-1-A1), CD19(1D3), IgM(ll/41), CD38(90), CD138(281-2), Ter-119 (Ter-119), CD3 (G4.18), CD90.2 (Thy1.2), CD4 (GK1.5), CD8 (53-6.7), TCRβ (H57-597) and CD25 (PC61.5), and antibody for human CD8 (HIT8a; BD Bioscience), were used. Antibodies were purchased from eBioscience unless otherwise specified. Flow cytometry was performed using a FACSCalibur instrument (BD Bioscience) and FlowJo software ver. 7.6.5 (Tree Star Inc.).

Histological analysis

Formalin-fixed and paraffin-embedded tissues were stained with hematoxylin and eosin. For immunostaining, anti-Bcl6 (N-3; Santa Cruz), anti-human CD8 (PAB2495; Abnova) and anti-GFP (ab290; Abcam) antibodies were used. Biotinylated peanut agglutinin (PNA; Vector Laboratories) was used to detect germinal center B cells.

Western blot analysis

Anti-Myc (#9402; CellSignaling Technology), anti-Bcl2 (3F11;PharMingen), anti-Ccnd1(5D4; IBL) and anti-tubulin (DM1A; Sigma) antibodies were used.

Analyses of the clonality of cells and somatic hypermutation.

For analysis of the clonality of lymphoma and somatic hypermutation of associated immunoglobulin genes, genomic DNA isolated from GFP+hCD8+ cells was subjected to PCR using primers that detect VDJ regions from immunoglobulin heavy chain genes, as described in the literature [11][12]. Combinations of forward (VHA, VHE or VHG) and reverse (JH4 intron, JH1D, JH2D, JH3D or JH4D) primers were used. The resulting PCR products were gel purified, cloned into pCR4-TOPO vector (Invitrogen) and sequenced. VH gene usage and VDJ recombination were analysed using IgBLAST （http://www.ncbi.nlm.nih.gov/igblast/) and IMGT/V-QUEST (http://www.imgt.org/ IMGT_vquest/share/textes/), respectively. The IgH gene sequence was compared with germline DNA sequences to determine the frequencies of somatic hypermutation. For analysis of the clonality of T cells, PCR-mediated amplification of the Dβ2-Jβ2 fragment was performed, as described in the literature [13].

Statistical analysis

Kaplan-Meier analysis and the log-rank test were performed using JMP 10.0.0 software (SAS Institute Inc.).

Detection of mutations in the Notch1 gene

Mutations in the Notch1 gene were detected as previously described [14].

Results and discussion

Generation of B cell neoplasm using *in vitro*-induced germinal center B cells.

In an effort to transduce genes into mouse germinal center B cells, we utilized *in vitro*-induced germinal center B cells (iGCB) [7] as a target of retroviral infection. B220+ B cells were isolated from mouse spleen, cultured with a stromal cell layer that expressed mouse CD40 ligand and mouse Baff for 4 days in the presence of IL4, and subsequently cultured for 2 days in the presence of IL21. Prior to the initiation of culture, B220+ B cells were positive for CD19 and IgM or IgD, but negative for GL7, Fas and B7-1 (Fig. 1A), and were thereby compatible with a naïve B cell phenotype. After 6 days of culture, the cells became negative for IgM/IgD, and positive for GL7, Fas and B7-1 (Fig. 1B), which was compatible with a germinal center B cell phenotype [7].

We therefore made use of this culture system for the retroviral transduction of genes. Given that “double hit” B cell lymphomas involving *Myc* and *Bcl2* are associated with poor prognosis in humans [6], we chose this combination of genes for the retroviral transduction and expected an aggressive lymphoma to develop as proof of the principles underlying our gene transduction system for the generation of lymphoma models. Retroviruses were infected into cells on the 5th and 6th days after initiation of the co-culture. Retroviruses were engineered to co-express GFP or an extracellular domain of human CD8 (hCD8) as surrogate markers for expression of Myc and Bcl2, respectively, thus facilitating identification of cells transduced with the respective gene. *GFP*-only virus was included as a control. Following infection with retroviruses, *GFP*-only-infected cells were B7-1-positive (+) with ~70% of cells being IgG1+, a phenotype comparable to GFP-negative (-) cells in the

same culture, although the degree of expression of IgG1 varied from experiment to experiment (Supplementary Fig.1). In the case of cells co-infected with retroviruses for Myc (GFP) and Bcl2 (hCD8), fractions corresponding to GFP+hCD8+, GFP+hCD8-, GFP-hCD8+ and GFP-hCD8- comprised 18–32% (Fig. 1C). The expression of CD19, B7-1, IgG1 and IgM was comparable between GFP+ and GFP- fractions, and comparable to that of GFP-only-infected cells (Fig. 1C). Furthermore, the expression was also comparable among the four fractions defined by GFP and hCD8 in an independent experiment (Supplementary Fig. 1).

We then transplanted the gene-transduced iGCB cells into mice. Our initial experiments made use of immune-deficient mice as recipients. To this end, a mixture of the four fractions, generated as a result of infection with retroviruses for Myc(GFP) and Bcl2(hCD8), was intraperitoneally transplanted into NSG mice. GFP-only-infected control cells were similarly transplanted. Although mice did not show apparent signs of disease after four weeks, they were sacrificed to examine the transplanted cells. While *GFP*-only-infected cells were virtually undetectable, *Myc/Bcl2*-infected cells were readily indentified, and indeed almost all B220+ cells in mice were doubly positive for GFP and hCD8, and indicative of Myc- and Bcl2-co-expressing cells (Fig. 2A). Although the cells largely lost expression of GL7 and Fas, B7-1 was retained (Fig. 2A). Cytospin preparations of BM and spleen cells revealed the presence of large lymphoid cells harboring atypical nuclei with prominent nucleoli (Fig. 2B). In order to determine the tumorigenicity of the *Myc/Bcl2* doubly transduced cells, we isolated the cells from the spleen of the primary recipient and intravenously transplanted these cells into immune-competent syngeneic mice. Secondary recipient mice succumbed to lymphoma within 2 weeks following transplantation and exhibited enlargement of lymph nodes (LN), spleen and thymus (Fig. 2C). Diffuse infiltration

of atypical large lymphoid cells was noted in LN (Fig. 2D) and spleen, and the histological findings were compatible with diffuse large lymphoma. The presence of Myc+Bcl2+ cells predominated in these organs (data not shown).

Finally, we employed immune-competent syngeneic hosts as primary recipients in order to confirm the observation made using immune-deficient mice. Intravenous transplantation of *Myc*- and *Bcl2*-infected cells killed 4 of the 5 mice 30–44 days following transplantation (Fig. 3A). The remaining mouse was scarified 39 days following transplantation and exhibited enlarged LN, spleen and thymus (Fig. 3B), with the presence of atypical large lymphoid cells predominating in various organs including LN, liver and lung. Histological findings were compatible with diffuse large lymphoma (Figs 3C and 3D). Flow cytometric analysis of spleen cells revealed the predominance of GFP(Myc) and hCD8(Bcl2) doubly expressing cells, with GFP+hCD8- being present as a minor population and GFP-hCD8+ being virtually undetectable (Fig. 3E). Analyses of cells in LN and thymus yielded a similar result to that obtained from spleen cells. Thus, although transplanted cells comprised a mixture of cells transduced with *Myc* and/or *Bcl2*, *Myc*- and *Bcl2*- doubly transduced cells acquired a growth advantage over singly-infected cells. Taken together, these findings reflect the synergy of the two genes in the development of lymphoma. The predominant cells were B220+CD19+ B cells of an IgG1-type (Fig. 3E).

In an independent experiment, detailed analysis of lymphoma cells in spleen and the use of immunostaining (Supplementary Fig. 2) revealed that (1) secondary follicles were enlarged, (2) lymphocytes residing in the enlarged follicles were morphologically compatible with centrocytes and centroblasts, and (3) GFP+hCD8+ lymphoma cells in the follicles were positive for Bcl6 and PNA staining, and therefore compatible with germinal center B cells. However, most GFP+hCD8+ lymphoma cells morphologically indistinguishable from those

residing in follicles were seen in the red pulp, and this finding is compatible with a diagnosis of DLBCL with follicular colonization. Despite bearing a resemblance to lymphoma cells in follicles, lymphoma cells in the red pulp were negative for Bcl6 and PNA staining, suggestive of non-GCB cells. The fact that there were two different components in the developed lymphoma was additionally confirmed by flow-cytometric analysis, which showed that only small numbers of GFP+hCD8+ cells were positive for the GCB markers GL7 and Fas (Supplementary Fig. 3). Coupled with negativity for plasma cell markers CD138/CD38 (Supplementary Fig. 3), these findings suggest that the lymphoma cells in the red pulp are post-germinal center B cells, which are considered counterparts of many types of lymphomas developing in humans [15].

Analysis of the clonality of evolved lymphoma through PCR-mediated amplification of the VDJ region of IgH and sequencing revealed the presence of a single major clone that was not accompanied by somatic hypermutation (SHM) (Supplementary Fig. 4). Reasons for the absence of SHM in our modeled neoplasm, despite representing post-germinal center B cells, are not clear from the present study, but likely reflect very low activity of AID in the *in vitro*-induced GCB cells [7] and the absence of antigenic stimulation in our mice, both of which otherwise normally induce SHM in B cells. Importantly, however, *in vitro*-induced GCB cells are known to differentiate into memory B and plasma cells following transplantation *in vivo,* the capacity of which is the hallmark of normal GCB cells [7]. SHM is generally thought to be one of the critical components that cause deregulated expression of genes such as PIM1[16] and Bcl6 [17], which substantially contribute to lymphomagenesis [18][19]. Although our analysis of clonality and SHM was conducted in a single diseased mouse, the lack of SHM in our modeled lymphoma suggests the lack of involvement of SHM-mediated gene deregulation in the development of lymphoma. The monoclonal nature

of the evolved lymphoma (Supplementary Fig. 4) nevertheless suggests the requirement of additional genetic or epigenetic abnormality, in addition to overexpression of Myc and Bcl2, for lymphoma development. Elucidation of such additional abnormality awaits further investigation.

Generation of T cell neoplasm using *in vitro*-induced T cells

In a similar initiative, we sought to establish an *in vitro* culture system that allows transduction of genes into T cells. To this end, we used T cells induced from immature hematopoietic cells that were cultured with an OP9-Dl1 stromal layer in the presence of Flt3-ligand and IL-7 [9]. The fraction of cells (%) that express CD4 and/or CD8 was maximized around 21 days after initiation of the culture (Fig. 4A), and the highest efficiency of gene transduction was achieved when cells were infected with retrovirus on day 15 after initiation of the culture (Supplementary Fig. 5). Cells infected with GFP-only control virus were able to differentiate into CD4 and/or CD8 cells with an efficiency comparable to that of *GFP*-uninfected cells (Fig. 4B), although the possibility that retroviral infection affects differentiation cannot be entirely excluded. Lentivirus was inefficient in transducing genes into T cells in our culture system (Supplementary Fig. 6).

Given the synergism of Myc and Bcl2 for the development of B cell lymphoma (Figs. 2 and 3), and our previous observation that Ccnd1 significantly increases the incidence of B cell neoplasm [8], we tested whether combinations of Myc, Bcl2 and Ccnd1 could induce T cell neoplasm utilizing the T cells induced *in vitro* as described above as a target of gene expression. Our investigation of gene expression data (GSE19069) made available by Iqubal et al. [20] additionally shows the presence of peripheral T cell lymphoma cases associated with concomitant over-representation of *MYC, BCL2* and *CCND1* (and/or

CCND3) (Supplementary Fig. 7). Thus, cells were infected with retrovirus that co-expresses Myc and Bcl2 (MSCV-*Bcl2*-pgk-*Myc*-ires-GFP: Supplementary Fig. 8) alone or in combination with retrovirus for Ccnd1 (MSCV-Ccnd1-ires-human CD4) on day 15 after initiation of the co-culture, and intravenously transplanted (0.7–1.0 x 10^7 cells) into lethally irradiated syngeneic hosts, along with radioprotective bone marrow cells. All 6 mice transplanted with *Bcl2/Myc/Ccnd1*-transduced T cells became moribund or died within 48 days after the transplantation. In contrast, only 3 of the 6 mice transplanted with *Bcl2/Myc*-transduced T cells became moribund or died, and the latency was significantly delayed compared with that of mice transplanted with *Bcl2/Myc/Ccnd1*-transduced cells (Fig. 5A). One of the two mice transplanted with *GFP* only-transduced cells was electively sacrificed 28 days after the transplantation and was without detectable GFP-positive cells (data not shown), suggesting that *GFP*-only transduced cells do not grow efficiently *in vivo*. The other mouse transplanted with *GFP*-only-transduced cells and 3 mice transplanted with *hCD4* only-transduced cells (all considered controls) showed no sign of disease at least until 120 days after the transplantation (Fig. 5A).

Diseased mice that received a transplant with *Bcl2/Myc/Ccnd1*-transduced T cells exhibited enlarged thymus, spleen and lymph nodes (n=2) (Fig. 5B), which were accompanied by diffuse infiltration of atypical large lymphoid cells, and the histological findings were compatible with diffuse large lymphoma (Fig. 5B). The remaining 4 mice that died also exhibited enlarged spleen upon autopsy. Flow-cytometric analysis of cells in bone marrow, thymus, spleen and lymph nodes in the diseased mice revealed that at least 70% of cells were positive for both GFP and hCD4, indicating the predominance of *Myc/Bcl2/Ccnd1*-cotransduced cells (Fig. 5C). The predominant cells were CD4 single-positive or CD4/CD8 double-positive T cells. The presence of two populations

regarding hCD4 expression in some organs likely reflect polyclonal nature of the neoplasm (description follows). Upon secondary transplantation of spleen cells, all 6 mice (two experiments employing 3 mice each) succumbed to the CD4+ T cell malignancy 18–48 days after the transplantation. Given the predominance of CD4 single-positive T cells in bone marrow, spleen and lymph nodes of the secondary recipient mice albeit CD4+CD8+ T cells contributing to neoplasm in thymus (Fig. 5D), we sought to determine whether the CD4+cells are able to propagate tumor in mice. Accordingly, column-purified CD4+ cells from the spleen of a primary recipient mouse were transplanted into secondary mice. Results showed that the secondary mice succumbed to CD4 single-positive T cell malignancy (Fig. 5E) 33–35 days following transplantation (n=3). Similarly, CD4+ cells purified from the secondary mice also propagated tumor in tertiary recipient mice (data not shown). Although the incidence of tumor was lower and latency was prolonged compared with that of *Myc/Bcl2/Ccnd1*-cotransduced cells (Fig. 5A), *Myc/Bcl2*-cotransduced cells also elicited CD4+ tumors following transplantation into mice, which were accompanied by enlargement of thymus, spleen and lymph nodes, and the histological findings were compatible with diffuse large lymphoma (Supplementary Fig. 9) . Upon secondary transplantation, these cells elicited tumor death 40–41 days after the transplantation (n=3). Although exons 26, 27 and 34 of the mouse *Notch-1* gene are often mutated in T cell malignancy in mice [21][22][10], we did not detect such mutations following sequencing of cDNA obtained from aroused tumors. The polyclonal nature of the evolved tumors, as evidenced by PCR analysis of Dβ2-Jβ2 rearrangements (Supplementary Fig. 10), the maintenance of expression of Myc, Bcl2 and Ccnd1 (Supplementary Fig. 11), as well as the lack of Notch1 mutation and a short latency, suggest that a combination of Myc, Bcl2 and Ccnd1 is sufficient for the development of T cell neoplasm generated by the use of our

culture system. The presence of dominant clones in some mice may reflect a growth advantage of the selected clones, but the underlying mechanisms are not clear from the present study (Supplementary Fig. 10).

Overall, our study presented here demonstrates the utility of our gene transduction system that allows rapid analysis of the role of gene combinations in the development of B or T cell neoplasm *in vivo*. Although production of mouse models of lymphoid malignancy using retrovirus transduction is not unprecedented, methods hitherto reported are for the production of neoplasm of plasma cells and precursor B cells. Largaespada et al. [23] injected retrovirus for *ABL-MYC* into mice to obtain neoplasm of terminally differentiated plasma cells. They then generated plasma cell neoplasm models by retroviral transduction of activated B cells with *ABL-MYC* in a short-term *in vitro* culture [24], while Nakagawa et al. [8] generated precursor B cell neoplasm by the *in vitro* retroviral transduction of fetal liver-derived precursor B cells. In contrast, we induced germinal center B cells ex vivo, and used the cells as a target of retroviral gene transduction. Importantly, the neoplasm thus obtained is that of matured B cells and not of plasma cells or precursor B cells, and corresponds to germinal center and post-germinal center B cells. The phenotype of neoplasms thus obtained is therefore distinct from those reported by Largaespada and Nakagawa. Although Eμ-*Myc* transgenic mice are widely used for lymphoma research, the lymphomas largely comprise precursor B cells (pre-B cells in ~50% and a mixture of pre-B and B cells in ~30% of cases) [2], which are usually not seen in humans [15]. In contrast, our model represents lymphoma of matured B cells. Additionally, we established a method for the generation of T cell neoplasm. Our method therefore could complement studies using time-consuming and costly investigations such as those employing transgenic and knock-in

technologies, and would facilitate progress in the area of lymphoma research.

Authorship and disclosure

K.A., Y.M-K. and S.T. conceived the study, performed experiments, analyzed data, and wrote the paper. K.O. performed histological analysis. M.S-K. analyzed gene expression data. K.K., N.Y., T.S and M.S. contributed to the discussion and data analysis.

Conflict of interest disclosure

The authors declare no competing financial interests.

Acknowledgements

We thank Ms. Seiko Sato for help with animal husbandry, and Kyoko Hirano for assistance. This work was supported by a Health Labour Sciences Research Grant from The Ministry of Health, Labour and Welfa**re** (S.T., K.K., K.O. and M.S.**),** a Grant-in-Aid for Scientific Research from The Ministry of Education, Culture, Sports, Science and Technology (M.S.), and a Grant-in-Aid for Scientific Research from the Japan Society for the Promotion of Science (S.T. and M.S.).

References

[1] Langdon WY, Harris AW, Cory S, Adams JM. The c-myc oncogene perturbs B lymphocyte development in E-mu-myc transgenic mice. Cell. 1986;47:11-18.

[2] Harris AW, Pinkert CA, Crawford M, Langdon WY, Brinster RL, Adams JM. The E mu-myc transgenic mouse. A model for high-incidence spontaneous lymphoma and leukemia of early B cells. The Journal of experimental medicine. 1988;167:353-371.

[3] Strasser A, Harris AW, Bath ML, Cory S. Novel primitive lymphoid tumours induced in transgenic mice by cooperation between myc and bcl-2. Nature. 1990;348:331-333.

[4] Lovec H, Grzeschiczek A, Kowalski MB, Moroy T. Cyclin D1/bcl-1 cooperates with myc genes in the generation of B-cell lymphoma in transgenic mice. The EMBO journal. 1994;13:3487-3495.

[5] Jacobs JJL, Scheijen B, Voncken JW, Kieboom K, Berns A, Van Lohuizen M. Bmi-1 collaborates with c-Myc in tumorigenesis by inhibiting c-Myc-induced apoptosis via INK4a/ARF. Genes & development. 1999;13:2678-2690.

[6] Aukema SM, Siebert R, Schuuring E, et al. Double-hit B-cell lymphomas. Blood. 2011;117:2319-2331.

[7] Nojima T, Haniuda K, Moutai T, et al. In-vitro derived germinal centre B cells differentially generate memory B or plasma cells in vivo. Nature Communications. 2011;2:465.

[8] Nakagawa M, Tsuzuki S, Honma K, Taguchi O, Seto M. Synergistic effect of Bcl2, Myc and Ccnd1 transforms mouse primary B cells into malignant cells. Haematologica. 2011;96:1318-1326.

[9] Schmitt TM, Zúñiga-Pflücker JC. Induction of T cell development from hematopoietic progenitor cells by delta-like-1 in vitro. Immunity. 2002;17:749-756.

[10] Tsuzuki S, Taguchi O, Seto M. Promotion and maintenance of leukemia by ERG. Blood. 2011;117:3858-3868.

[11] Ehlich A, Martin V, Muller W, Rajewsky K. Analysis of the B-cell progenitor compartment at the level of single cells. Current Biology. 1994;4:573-583.

[12] Sander S, Calado DP, Srinivasan L, et al. Synergy between PI3K signaling and MYC in Burkitt lymphomagenesis. Cancer Cell. 2012;22:167-179.

[13] Dumortier A, Jeannet R, Kirstetter P, et al. Notch activation is an early and critical event during T-Cell leukemogenesis in Ikaros-deficient mice. Molecular and cellular biology. 2006;26:209-220.

[14] O'Neil J, Calvo J, McKenna K, et al. Activating Notch1 mutations in mouse models of T-ALL. Blood. 2006;107:781-785.

[15] Shaffer III AL, Young RM, Staudt LM. Pathogenesis of B cell lymphomas. Annual Review of Immunology. 2012;30:565-610.

[16] Pasqualucci L, Neumeister P, Goossens T, et al. Hypermutation of multiple proto-oncogenes in B-cell diffuse large-cell lymphomas. Nature. 2001;412:341-346.

[17] Pasqualucci L, Migliazza A, Fracchiolla N, et al. BCL-6 mutations in normal germinal center B cells: evidence of somatic hypermutation acting outside Ig loci. Proceedings of the National Academy of Sciences. 1998;95:11816-11821.

[18] Kotani A, Kakazu N, Tsuruyama T, et al. Activation-induced cytidine deaminase (AID) promotes B cell lymphomagenesis in Emu-cmyc transgenic mice. Proceedings of the

National Academy of Sciences. 2007;104:1616-1620.
[19] Pasqualucci L, Bhagat G, Jankovic M, et al. AID is required for germinal center-derived lymphomagenesis. Nature genetics. 2007;40:108-112.
[20] Iqbal J, Weisenburger DD, Greiner TC, et al. Molecular signatures to improve diagnosis in peripheral T-cell lymphoma and prognostication in angioimmunoblastic T-cell lymphoma. Blood. 2010;115:1026-1036.
[21] Chiang MY, Xu L, Shestova O, et al. Leukemia-associated NOTCH1 alleles are weak tumor initiators but accelerate K-ras-initiated leukemia. The Journal of clinical investigation. 2008;118:3181-3194.
[22] Tremblay M, Tremblay CS, Herblot S, et al. Modeling T-cell acute lymphoblastic leukemia induced by the SCL and LMO1 oncogenes. Genes & development. 2010;24:1093-1105.
[23] Largaespada DA, Kaehler DA, Mishak H, et al. A retrovirus that expresses v-abl and c-myc oncogenes rapidly induces plasmacytomas. Oncogene. 1992;7:811-819.
[24] Largaespada DA, Jackson MW, Thompson NE, Kaehler DA, Byrd LG, Mushinski JF. The ABL-MYC retrovirus generates antigen-specific plasmacytomas by in vitro infection of activated B lymphocytes from spleen and other murine lymphoid organs. Journal of immunological methods. 1996;197:85-95.

Figure legends

Figure 1. Induction of germinal center B cells *in vitro* and retroviral gene-transduction.

(A) Flow cytometric analysis of spleen B cells prior to induction. (B) Flow cytometric analysis of iGCB cells. Note that IgM and IgD were down-regulated and germinal center-associated molecules (GL7, Fas and B7-1) were up-regulated. (C) Retroviral gene transduction into cells. Upper panels: retrovirus for GFP-only control was infected into cells during the induction period of GCB cells. Lower panels: retroviruses for Myc and Bcl2 that respectively co-express GFP and hCD8, as surrogate markers, were similarly infected into cells. Infected cells were analyzed for expression of the indicated molecules. No appreciable difference

was noted with respect to expression of differentiation-associated molecules regardless of gene-transduction.

Figure 2. Development of lymphoma in immune-deficient mice. (A) iGCB cells infected with retroviruses for Myc and Bcl2, as shown in Fig. 1C, were transplanted into an NSG mouse, and B220+ B cells in bone marrow (BM), spleen and liver were analyzed for the expression of GFP (representing Myc expression) and hCD8 (representing Bcl2), along with various germinal center-associated molecules. (B) May-Grunwald-Giemsa staining of cells in BM and spleen (x100 objective). (C) Gross anatomy of a C57BL/6 mouse secondarily transplanted with spleen cells shown in (A). Note enlarged lymph nodes (LN), spleen and thymus. (D) Hematoxylin and eosin staining of a lymph node (upper panels: x4 objective, lower panels: x40 objective).

Figure 3. Development of lymphoma in immune-competent mice. (A) A Kaplan-Meier curve for the probability of disease-free survival following transplantation of *Myc*- and *Bcl2*-co-transduced iGCB cells. Death or moribundity was considered an event. (B) Gross anatomy of a diseased mouse, which shows enlarged lymph nodes (LN), spleen and thymus. (C) May-Grunwald-Giemsa staining of cells in spleen and LN (x100 objective). (D) Hematoxylin and eosin staining of tissues (upper panels: x4 objective, lower panels: x40 objective). (E) Flow cytometric analysis of spleen cells for expression of GFP(Myc) and hCD8(Bcl2)(left), and the indicated B cell-associated molecules on GFP+ cells (right).

Figure 4. Establishment of an *in vitro* culture system that allows retroviral transduction of genes into T cells. (A) Differentiation of T cells from mouse fetal liver cells. Ter119-depleted

mouse fetal liver cells were cultured with an OP9/Dl1 stromal cell layer in the presence of Flt3-ligand and IL7. Expression of T cell-affiliated markers was analyzed by flow cytometry on the indicated days after initiation of the culture. Numbers shown represent percentages of respective fractions. (B) Differentiation of *GFP*-transduced cells. Cells infected with *GFP*-only retrovirus on the 15^{th} day after initiation of the culture were monitored for differentiation 6 days later. Differentiation potential of *GFP*-transduced cells appears comparable with that of GFP-negative untransduced cells.

Figure 5. Tumorigenicity of gene-transduced T cells *in vivo*. (A) A Kaplan-Meier curve representing disease-free survival, in which death and moribundity were considered events. Cells transduced with the indicated genes were intravenously transplanted ($0.7–1.0\times10^7$ cells) into syngeneic hosts. Mice transplanted with cells infected with viruses for GFP-only (n=2) and hCD4-only (n=3) were combined and considered a control group (n=5). The difference in probability of disease-free survival was statistically significant as estimated by the log-rank test. (B) Gross anatomy of a diseased mouse that received a transplant with *Bcl2/Myc/Ccnd1*-transduced cells. Note that the thymus (open triangles), spleen (filled triangles) and lymph nodes (circle) were enlarged. Histology (spleen and lymph nodes) is also presented (upper panels: x4 objective, lower panels: x40 objective). (C) Flow-cytometric analysis of a diseased mouse. Expression of GFP (representing expression of Bcl2/Myc) and human CD4 (representing expression of Ccnd1) in cells of various organs are presented, along with expression of T cell-affiliated markers on GFP+ cells. Note that GFP+hCD4+ cells predominated in all organs analyzed. (D) Flow-cytometric analysis of a diseased mouse that received a transplant with spleen cells of a primary recipient mouse. (E) Flow-cytometric analysis of a diseased mouse that received a transplant with CD4+ cells

purified from spleen cells of a primary recipient mouse. Note that CD4+CD8- cells predominated in the organs of the secondary recipient mouse.

Figure 1

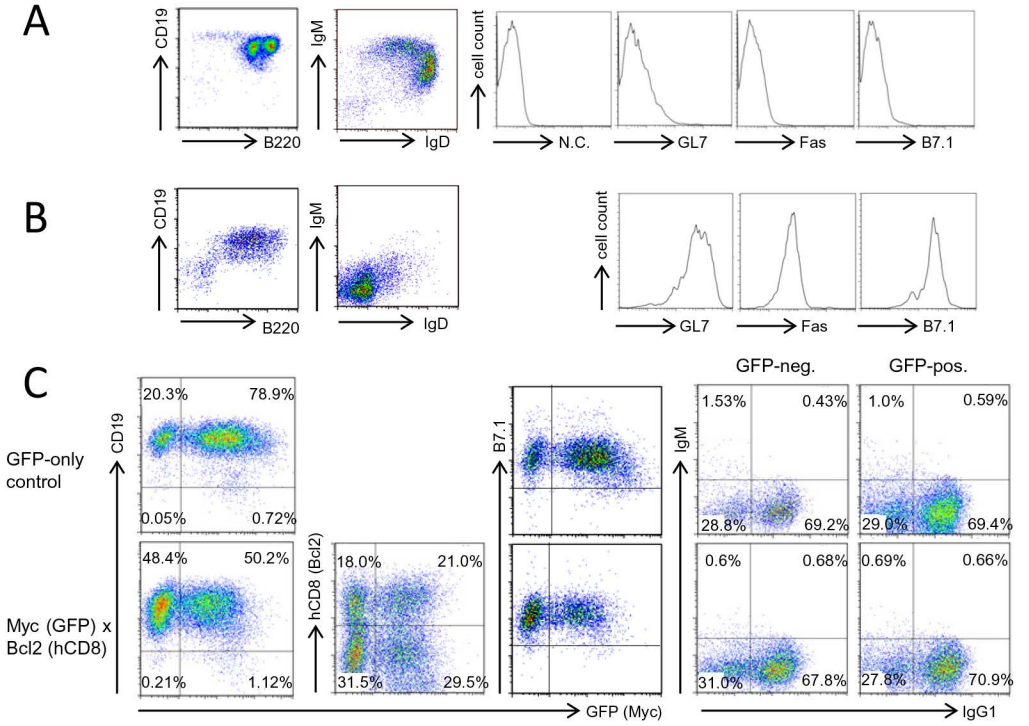
A
CD19
B220
IgM
IgD
cell count
N.C.
GL7
Fas
B7.1
B
CD19
B220
IgM
IgD
cell count
GL7
Fas
B7.1
C
GFP-neg.
GFP-pos.
GFP-only control
Myc (GFP) x Bcl2 (hCD8)
CD19
hCD8 (Bcl2)
B7.1
IgM
GFP (Myc)
IgG1
20.3%
78.9%
0.05%
0.72%
48.4%
50.2%
0.21%
1.12%
18.0%
21.0%
31.5%
29.5%
1.53%
0.43%
28.8%
69.2%
1.0%
0.59%
29.0%
69.4%
0.6%
0.68%
31.0%
67.8%
0.69%
0.66%
27.8%
70.9%

Figure2

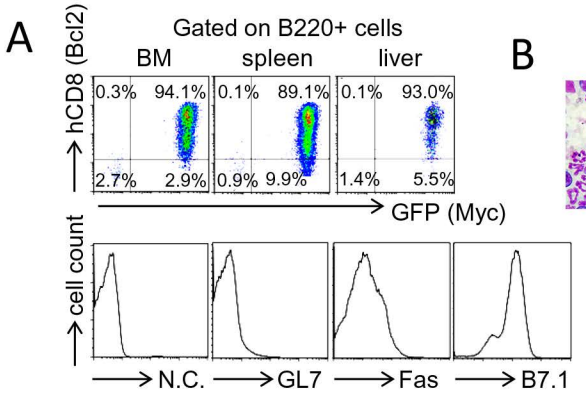
A
Gated on B220+ cells
BM
spleen
liver
hCD8 (Bcl2)
0.3%
94.1%
2.7%
2.9%
0.1%
89.1%
0.9%
9.9%
0.1%
93.0%
1.4%
5.5%
GFP (Myc)
cell count
N.C.
GL7
Fas
B7.1

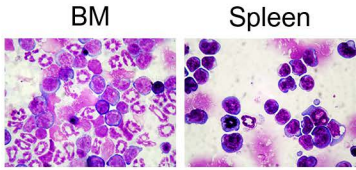
B
BM
Spleen

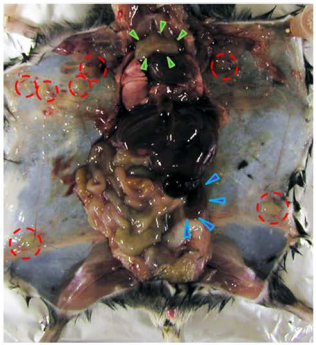
C

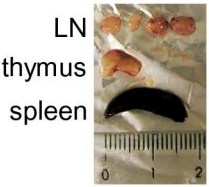
LN
thymus
spleen
0
1
2

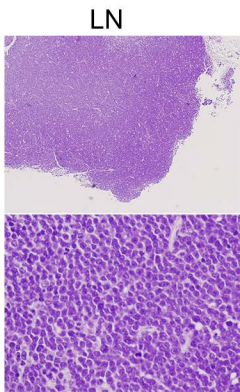
D
LN

Figure 3

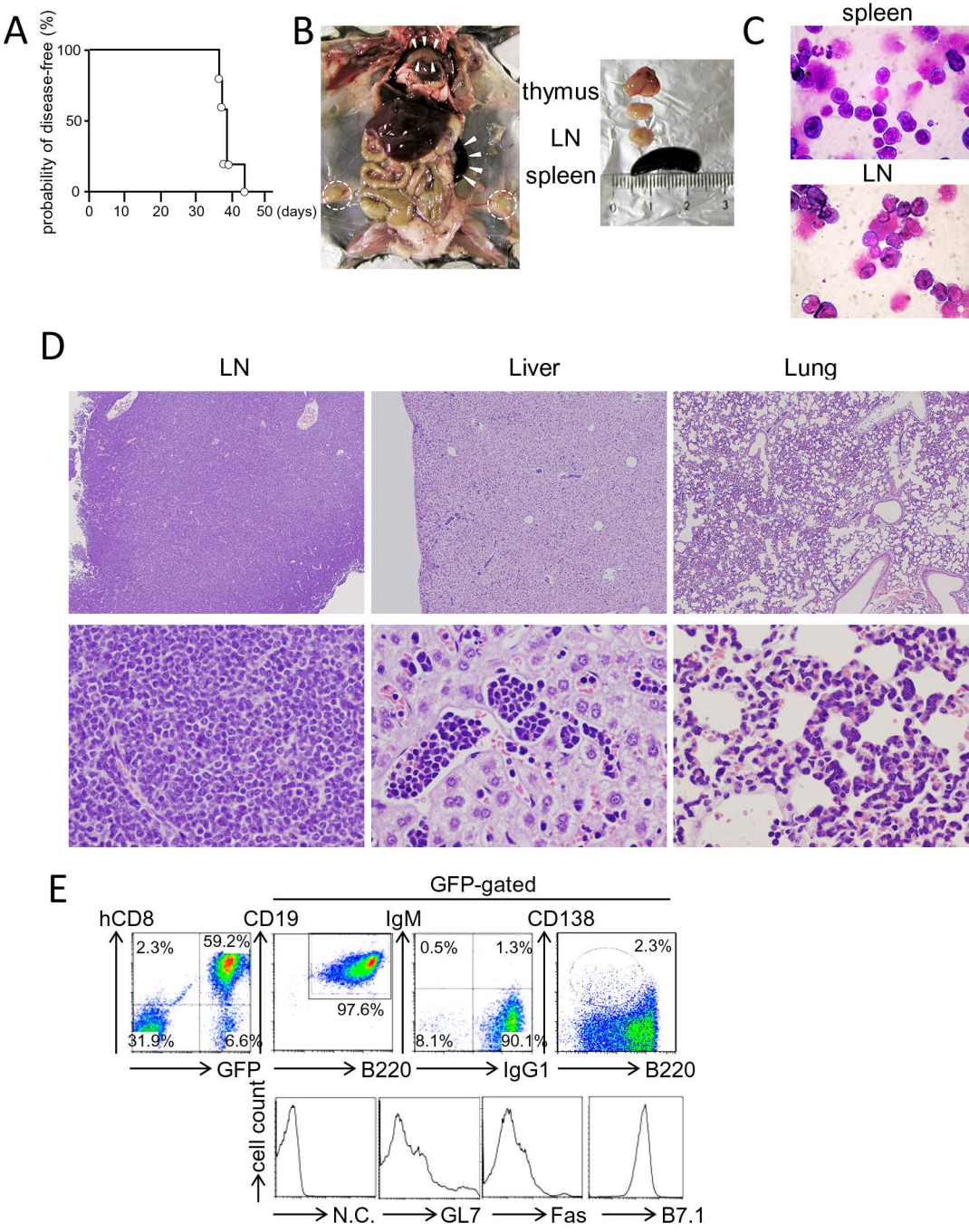
A
probability of disease-free (%)
100
50
0
0
10
20
30
40
50 (days)
B
thymus
LN
spleen
C
spleen
LN
D
LN
Liver
Lung
E
GFP-gated
hCD8
CD19
IgM
CD138
2.3%
59.2%
31.9%
6.6%
97.6%
0.5%
1.3%
8.1%
90.1%
2.3%
GFP
B220
IgG1
B220
cell count
N.C.
GL7
Fas
B7.1

Figure 4

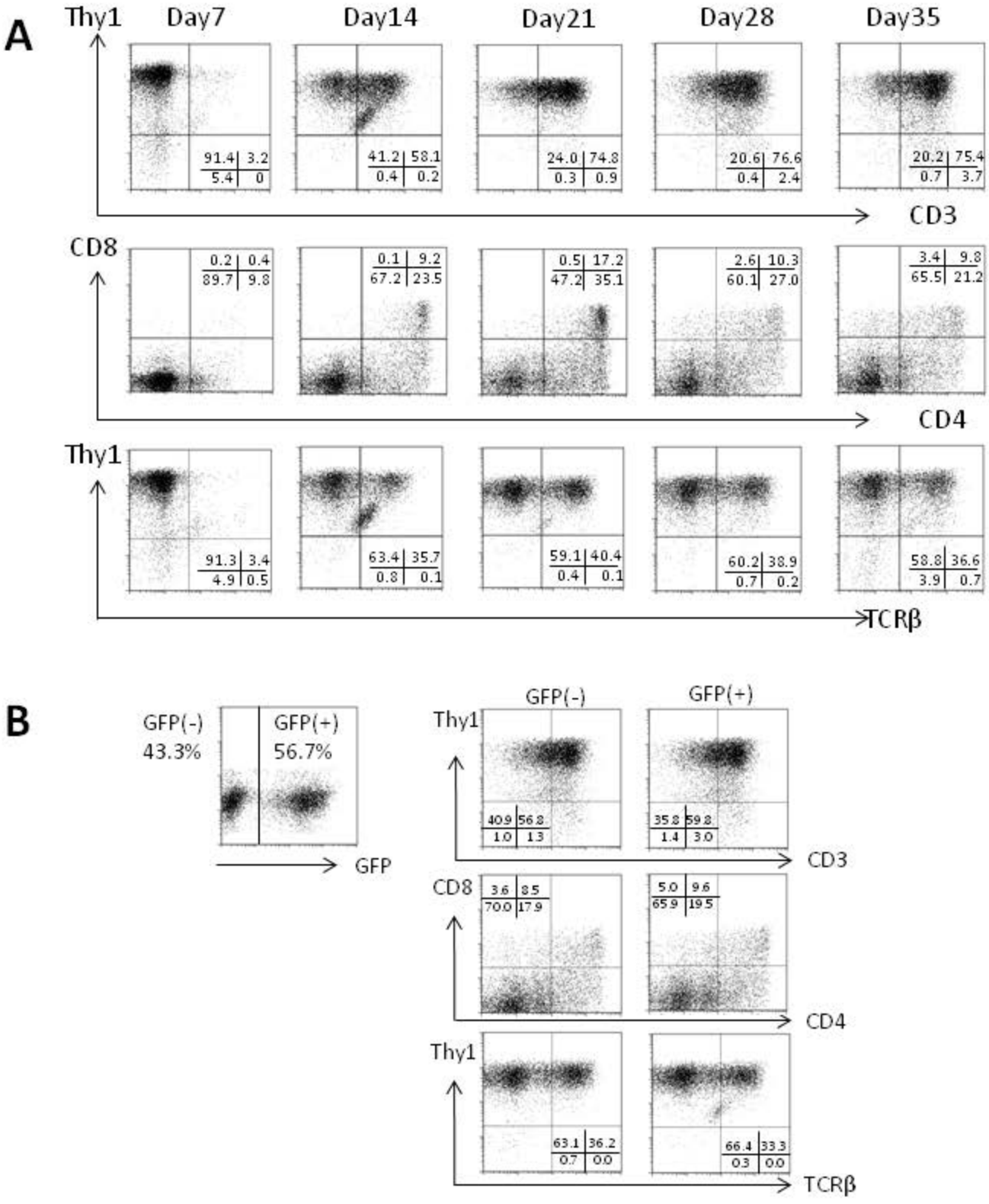
A
Thy1
Day7
Day14
Day21
Day28
Day35
91.4 3.2
5.4 0
41.2 58.1
0.4 0.2
24.0 74.8
0.3 0.9
20.6 76.6
0.4 2.4
20.2 75.4
0.7 3.7
CD3
CD8
0.2 0.4
89.7 9.8
0.1 9.2
67.2 23.5
0.5 17.2
47.2 35.1
2.6 10.3
60.1 27.0
3.4 9.8
65.5 21.2
CD4
Thy1
91.3 3.4
4.9 0.5
63.4 35.7
0.8 0.1
59.1 40.4
0.4 0.1
60.2 38.9
0.7 0.2
58.8 36.6
3.9 0.7
TCRβ
B
GFP(-)
43.3%
GFP(+)
56.7%
GFP
GFP(-)
GFP(+)
Thy1
40.9 56.8
1.0 1.3
35.8 59.8
1.4 3.0
CD3
CD8
3.6 8.5
70.0 17.9
5.0 9.6
65.9 19.5
CD4
Thy1
63.1 36.2
0.7 0.0
66.4 33.3
0.3 0.0
TCRβ

Figure 5

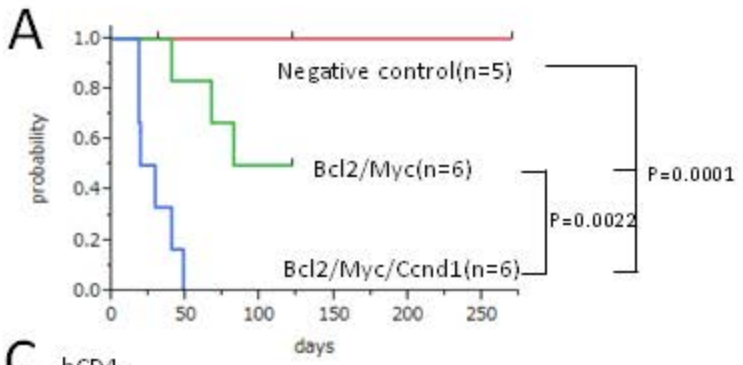
A
1.0
0.8
0.6
0.4
0.2
0.0
probability
0
50
100
150
200
250
days
Negative control(n=5)
Bcl2/Myc(n=6)
Bcl2/Myc/Ccnd1(n=6)
P=0.0001
P=0.0022

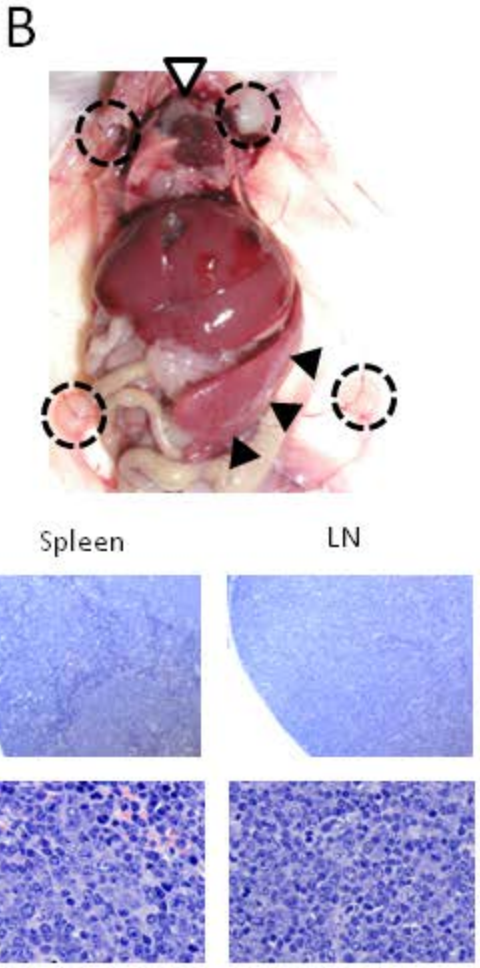
B
Spleen
LN

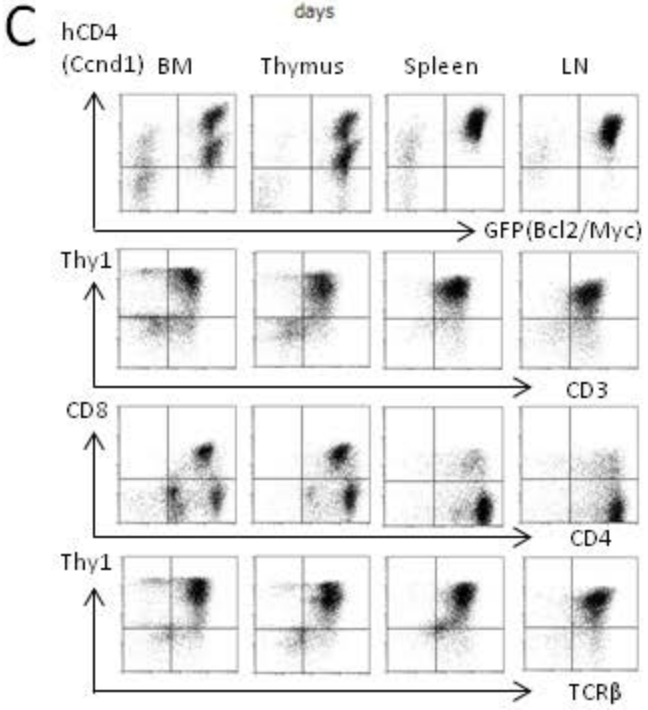
C
hCD4
(Ccnd1)
BM
Thymus
Spleen
LN
GFP(Bcl2/Myc)
Thy1
CD3
CD8
CD4
Thy1
TCRβ

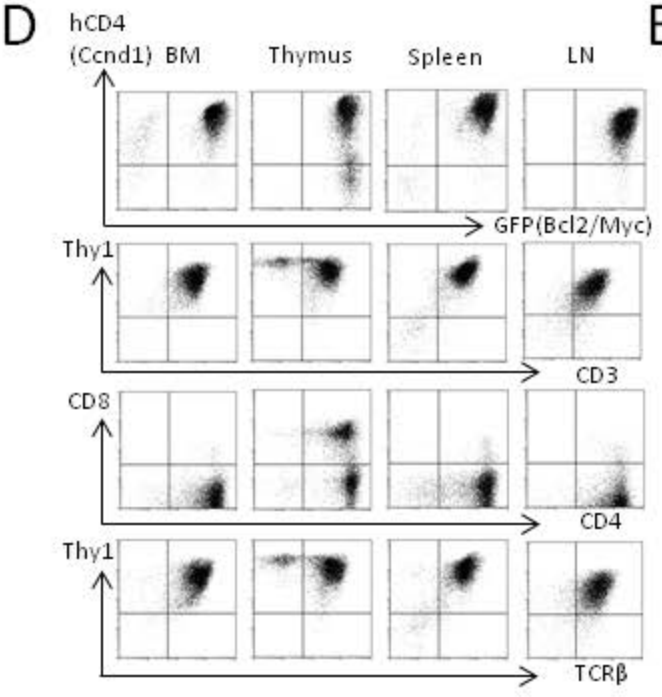
D
hCD4
(Ccnd1)
BM
Thymus
Spleen
LN
GFP(Bcl2/Myc)
Thy1
CD3
CD8
CD4
Thy1
TCRβ

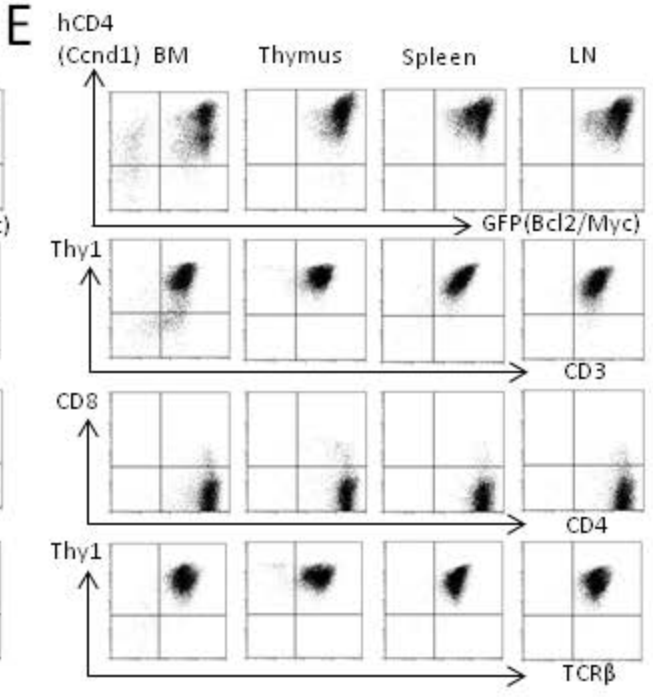
E
hCD4
(Ccnd1)
BM
Thymus
Spleen
LN
GFP(Bcl2/Myc)
Thy1
CD3
CD8
CD4
Thy1
TCRβ

Supplementary Figure Legends

Supplementary Fig. 1.

Flow cytometric analysis of Bcl2/Myc co-transduced iGCB cells before transplantation. Cells in the four fractions determined by positivity of GFP (representing Myc expression) and/or hCD8 (representing Bcl2 expression) were analyzed for expression of CD19, B7.1, IgM and IgG1.

Supplementary Fig. 2.

Histological analyses of spleens of mice. (A) Hematoxylin and eosin staining of spleens of normal (left) and diseased (right) mice with the indicated original magnification. (B) Staining of spleens of normal (left) and diseased (right) mice with anti-Bcl6, PNA, anti-GFP and anti-human CD8. Original magnifications are also presented.

Supplementary Fig. 3.

Flow cytometric analysis of the expression of Fas and GL7. (A) Spleen cells of a normal C57BL/6 mouse (left) and those of a mouse immunized thrice with sheep red blood cells (right). (B) iGCB cells in culture. (C) Spleen cells of a C57BL/6 mouse transplanted with Bcl2/Myc-co-transduced iGCB cells. Note that GL7+Fas+ cells that are considered germinal center B cells are evident in spleen of an immunized mouse (A; right) and iGCB cells in culture (B), but not in spleen cells of a normal mouse (A; left) and GFP+ lymphoma cells in spleen of a mouse transplanted with Myc- and Bcl2-co-transduced iGCB cells (C). Plasma cells defined by CD138+CD38+ were barely detected in the GFP+ fraction (C).

Supplementary Fig. 4.

Analysis of the clonality and somatic hypermutation of immunoglobulin genes of GFP+hCD8+ tumor cells purified from spleen of an affected mouse. (A) Electrophoresis of PCR products using VHA and JH4 intron primers showing a single band. ∗: non-specific band. (B) VH gene usage determined by the IgBLAST program. No somatic hypermutation was observed. (C) IgH VDJ rearrangement determined by the IMGT/V-QUEST program. Productive in-frame rearrangement carrying no somatic hypermutation was observed.

Supplementary Fig. 5.

Efficiency of retroviral transduction of a gene into T cells. Cells were infected with retrovirus for GFP on days 3, 9, 15, 21 and 27 after the initiation of culture, and monitored for expression of GFP every 3 days after the infection until the 30th day after the initiation of culture. Note that the highest efficiency of gene transduction was achieved when cells were infected on day 15 after initiation of culture.

Supplementary Fig. 6.

Comparison of infection into T cells between retrovirus and lentivirus. Cells were infected on the indicated days after the initiation of culture, and the % of transduced cells (represented by %GFP) was monitored 3-6 days later. The efficiency of lentiviral infection into K562 cells is also presented to show that the absence of lentiviral infection into T cells is not due to inefficient production of virus.

Supplementary Fig. 7.

Expressions of *MYC*, *BCL2* and *CCND1-3* in cases with peripheral T cell lymphoma. Gene

expression data (GSE19069) were used for clustering with Cluster 3.0 software (http://bonsai.hgc.jp/~mdehoon/software/cluster/). Arrows indicate cases with concomitant over-representation of *MYC*, *BCL2* and *CCND1*/2/*3*.

Supplementary Fig. 8.

Schematic drawings of retroviral plasmids (not to scale). Positions of primers used in Supplementary Fig. 11C are shown by arrows.

Supplementary Fig. 9.

Flow-cytometric analysis and histology of the organs of a mouse transplanted with T cells transduced with Myc and Bcl2.

Supplementary Fig. 10.

PCR analysis of the clonality of T cell neoplasms. The presence of more than one band for amplified Dβ2-Jβ2 fragments suggests oligo-clonality of evolved neoplasms. Note that the tail DNA exhibits only a single germ line band (indicated by an arrow head). 1st: primary recipient, 2nd: secondary recipient, 3rd: tertiary recipient, CD4+: a recipient of purified CD4+ cells. 1-2nd represents a mouse that received a graft from the 1-1st mouse. 2-2nd represents a mouse that received a graft from the 2-1st mouse. 2-3rd represents a mouse that received a graft from the 2-2nd mouse.

Supplementary Fig. 11.

Expression of Bcl2, Myc and Ccnd1 in neoplasm. (A) Tumor cells were analysed for the expression of various proteins. Analysis of tubulin expression was included to allow

comparison of loaded protein amounts. Normal thymus served as a control. (B) Relative amount of protein expressed, with that of a 1-1st mouse being set as 1.0. (C) RT-PCR analysis of the expression of retrovirally transduced Myc. The primer set 5'-GAAAAGGCCCCCAAGGTAGT-3' and 5'-TATGGTGGAAAATAACATATAGAC-3' (positions are shown in Supplementary Fig. 8) was used. Note that although Myc protein expression in some tumors is not dissimilar to that of normal thymus, RT-PCR analysis confirms the expression of transduced Myc. RT-: without reverse transcription, RT+: with reverse transcription. See the legend to Supplementary Fig. 10 for descriptions of 1-1st, 1-2nd, 2-1st, 2-2nd, 2-3rd and CD4+.

Supplementary Fig.1

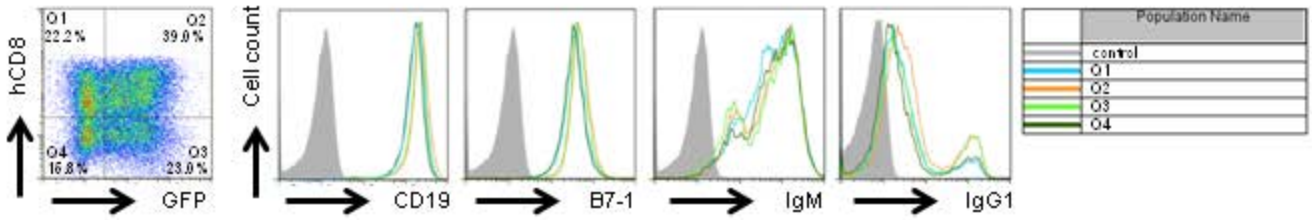

Supplementary Fig.2

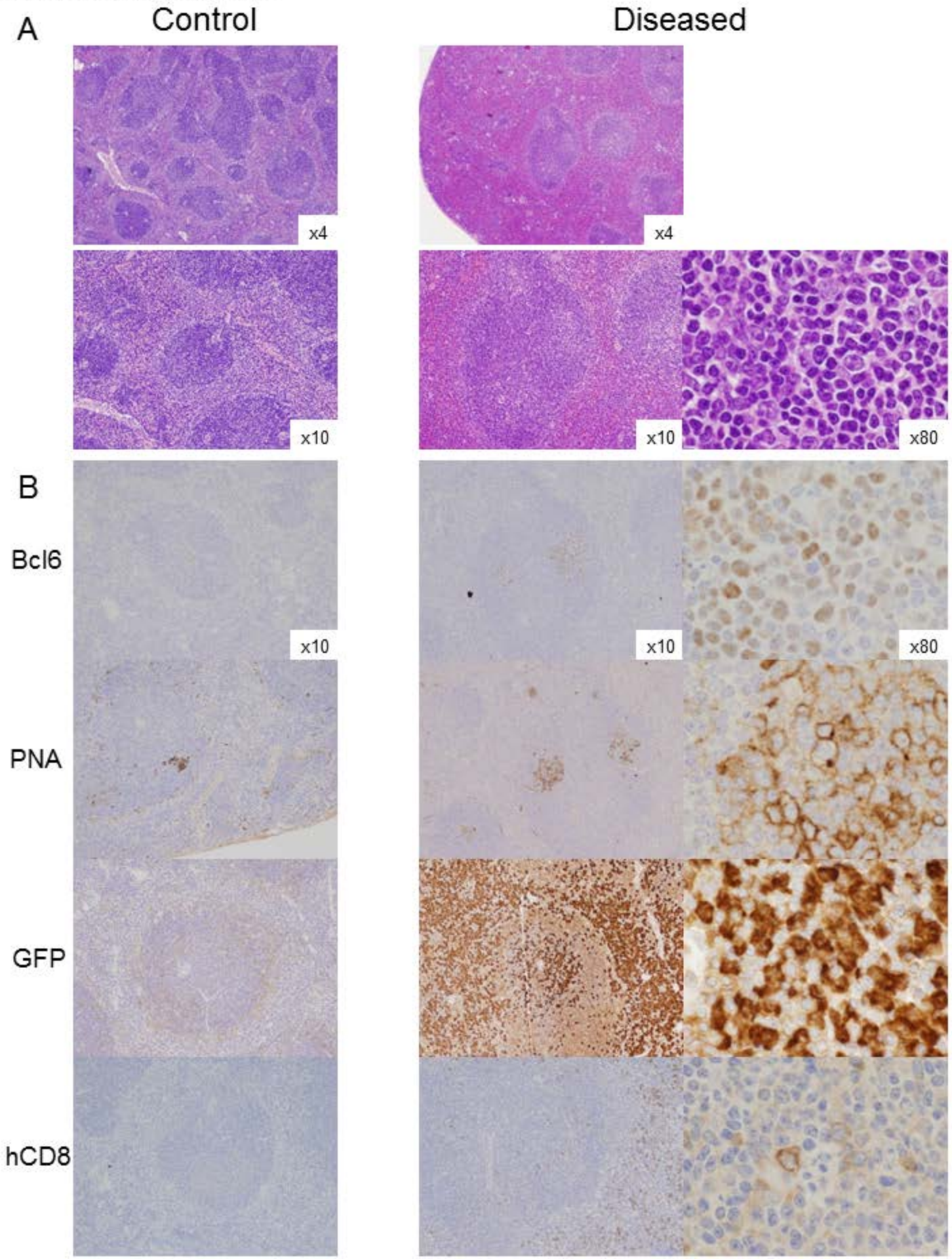

Supplementary Fig.3

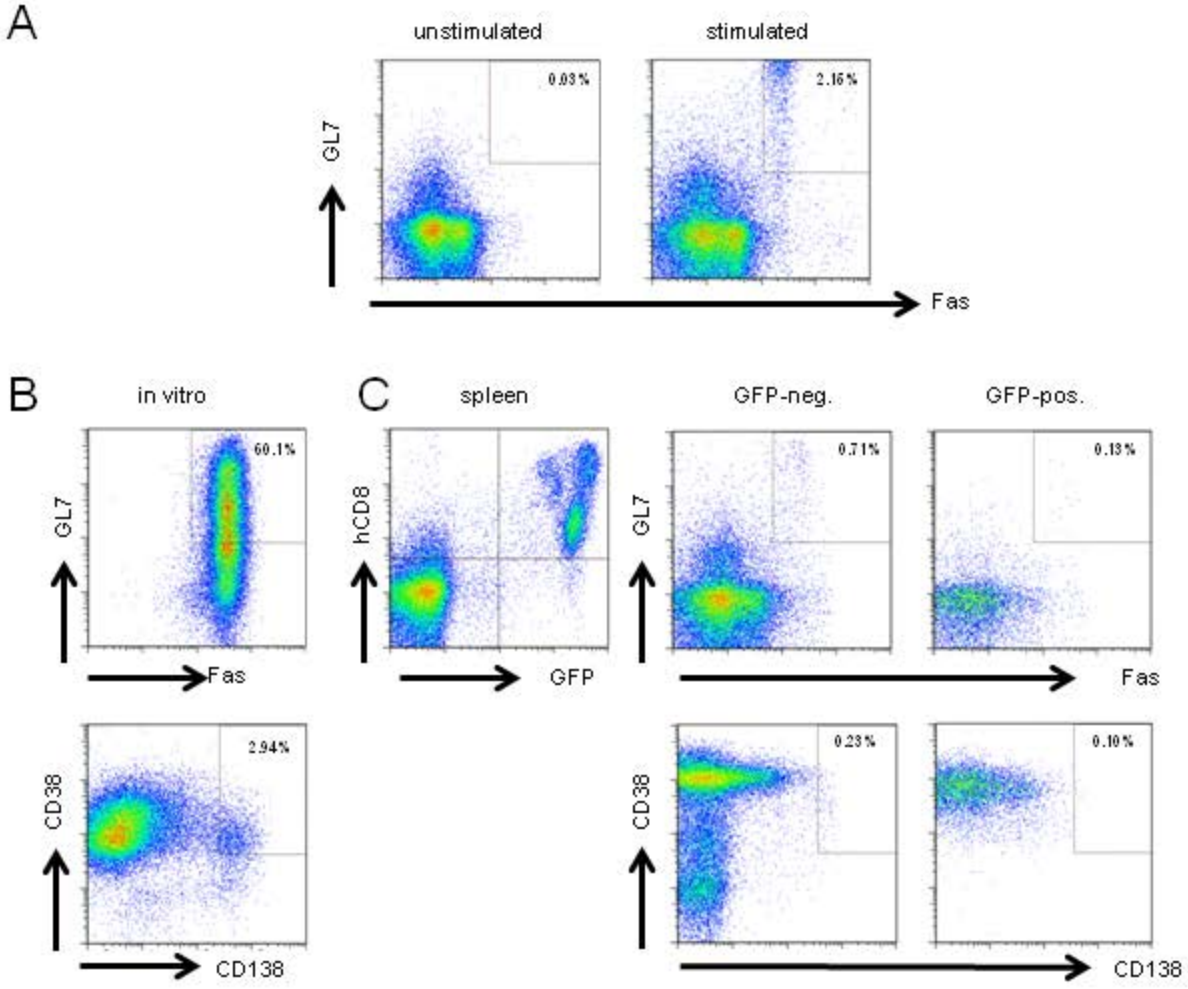

Supplementary Fig.4

A

B

```
                                                <----------FWR1----------><-----CDR1----><----------------FWR2---------------->
                                                 I  S  C  K  A  S  G  Y  S  F  T  G  Y  Y  M  N  W  V  K  Q  S  P  E  K  S  L  E  W  I  G
                        Query_1          1      ATATCCTGCAAGGCTTCTGGTTACTCATTCACTGGCTACTACATGAACTGGGTGAAGCAAAGTCCTGAAAAGAGCCTTGAGTGGATTGGA  90
V  100.0% (237/237)     IGHV1-42*01      58     ..............................................................................................  147
                                                 I  S  C  K  A  S  G  Y  S  F  T  G  Y  Y  M  N  W  V  K  Q  S  P  E  K  S  L  E  W  I  G
V  96.6% (229/237)      IGHV1-43*01      58     ..............................................C.................T.....................  147
V  92.0% (218/237)      IGHV1S30*02      49     ..............................................C.............G..C.A..G.....................  138

                                                <----------------------CDR2----------------------><-----------------------------------
                                                 E  I  N  P  S  T  G  G  T  T  Y  N  Q  K  F  K  A  K  A  T  L  T  V  D  K  S  S  S  T  A
                        Query_1          91     GAGATTAATCCTAGCACTGGTGGTACTACCTACAACCAGAAGTTCAAGGCCAAGGCCACATTGACTGTAGACAAATCCTCCAGCACAGCC  180
V  100.0% (237/237)     IGHV1-42*01      148    ..............................................................................................  237
                                                 E  I  N  P  S  T  G  G  T  T  Y  N  Q  K  F  K  A  K  A  T  L  T  V  D  K  S  S  S  T  A
V  96.6% (229/237)      IGHV1-43*01      148    ..........................G.....................G............A...........G..A............  237
V  92.0% (218/237)      IGHV1S30*02      139    ..A.........TA..A...........G.....................G.......................C..............G  228

                                                --------FWR3---------------------------------------------->
                                                 Y  M  Q  L  K  S  L  T  S  E  D  S  A  V  Y  Y  C  A  R  R  D  S  Y  A  M  D  Y  W  G  Q
                        Query_1          181    TACATGCAGCTCAAGAGCCTGACATCTGAGGACTCTGCAGTCTATTACTGTGCAAGACGGGATTCCTATGCTATGGACTACTGGGGTCAA  270
V  100.0% (237/237)     IGHV1-42*01      238    ..........................................................----------------------------------  294
                                                 Y  M  Q  L  K  S  L  T  S  E  D  S  A  V  Y  Y  C  A  R
V  96.6% (229/237)      IGHV1-43*01      238    ....................................T..................----------------------------------  294
V  92.0% (218/237)      IGHV1S30*02      229    ......G.....C.C.....................TTG..................----------------------------------  285
J  100.0% (50/50)       IGHJ4*01         5      ------------------------------------------------------------.....................  29
J  87.5% (35/40)        IGHJ2*02         9      ------------------------------------------------------------.....................  29
J  85.0% (34/40)        IGHJ2*01         9      ------------------------------------------------------------.....................  29

                                                 G  T  S  V  T  V  S  S
                        Query_1          271    GGAACCTCAGTCACCGTCTCCTCAG  295
J  100.0% (50/50)       IGHJ4*01         30     .........................  54
J  87.5% (35/40)        IGHJ2*02         24     ..C.....TC....A..........  48
J  85.0% (34/40)        IGHJ2*01         24     ..C...A.TC....A..........  48
```

C

V name	3'V-REGION	N1	D-REGION	N2	5'J-REGION	J name	D name	Vmut	Dmut	Jmut	Ngc
Musmus IGHV1-42*01	tgtgcaaga	cgg	.....gatt.....	c	....ctatgctatggactactgg	Musmus IGHJ4*01	Musmus IGHD2-4*01	0	0	0	4/4

Supplementary Fig.5

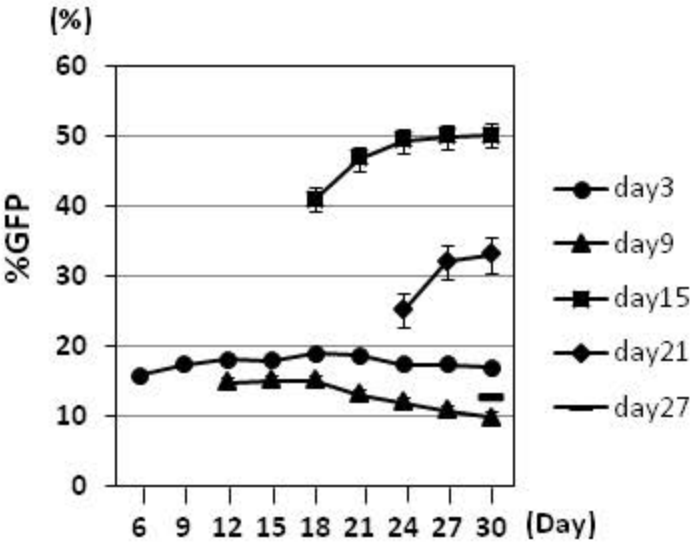

Supplementary Fig.6

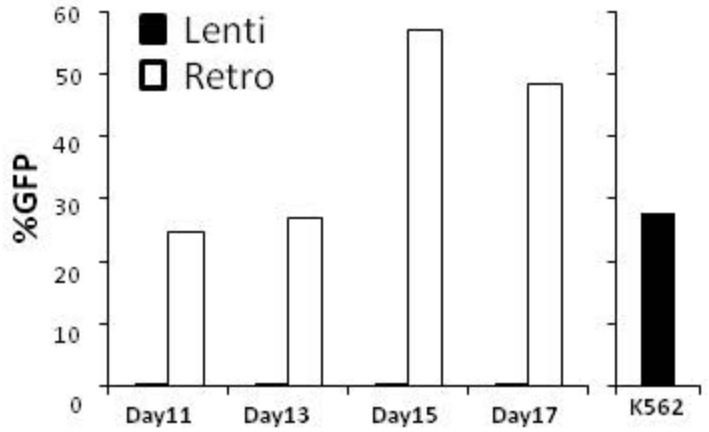

Supplementary Fig.7

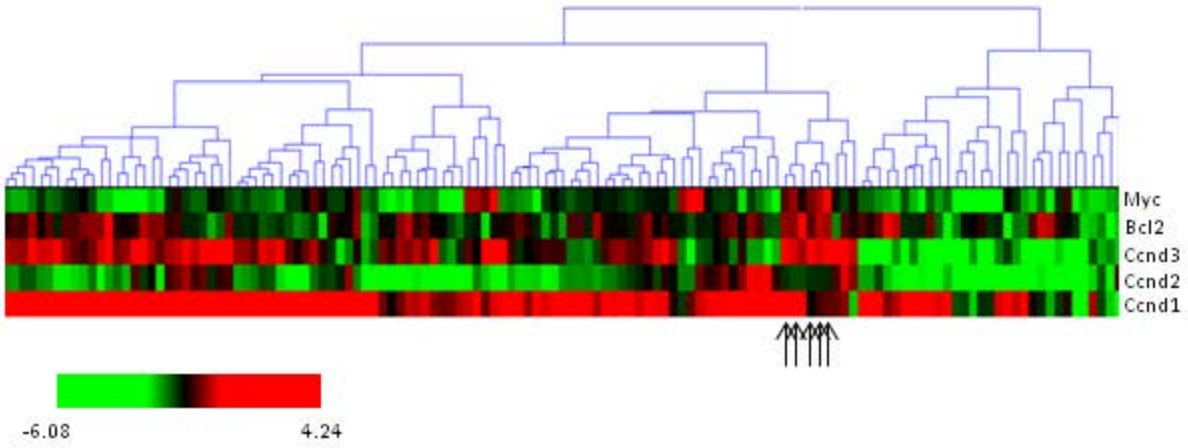

Supplementary Fig.8

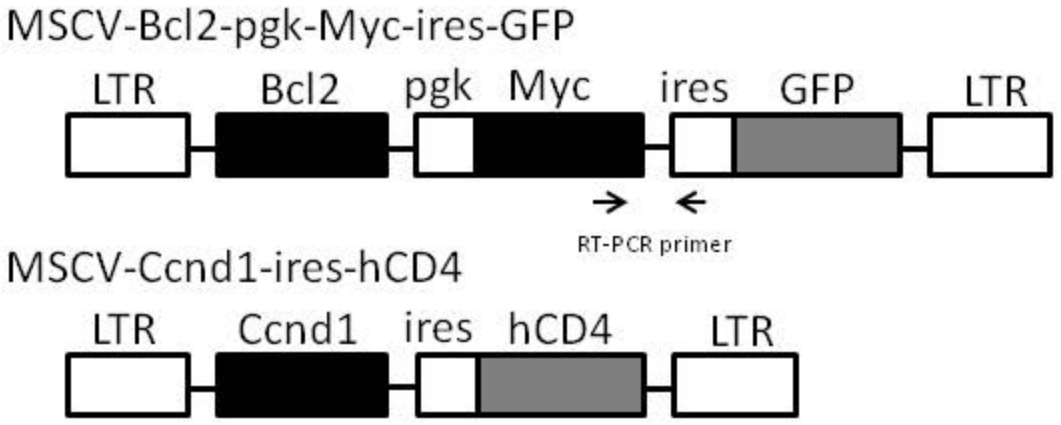

Supplementary Fig.9

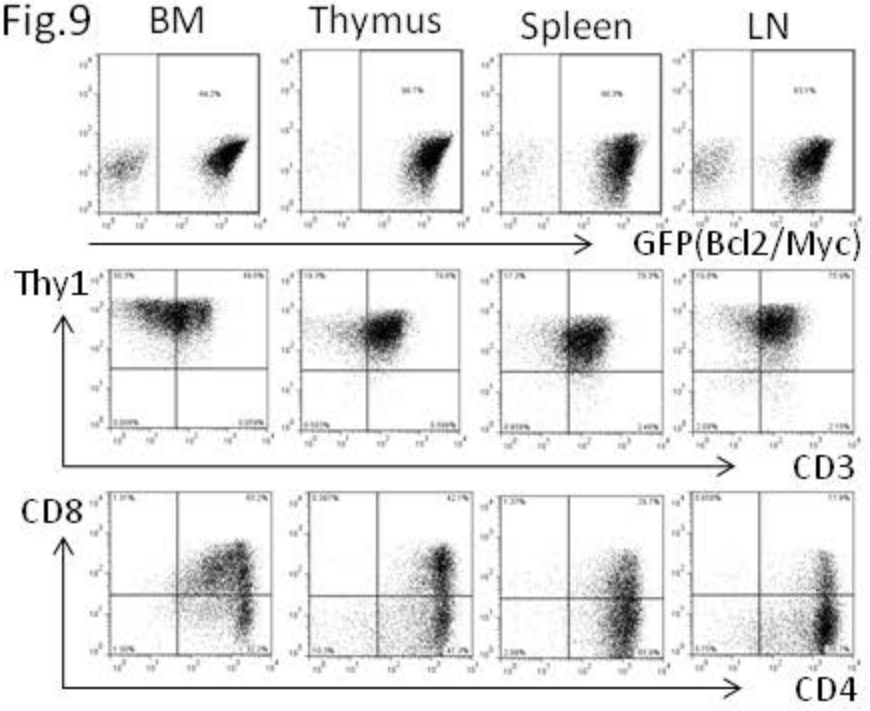

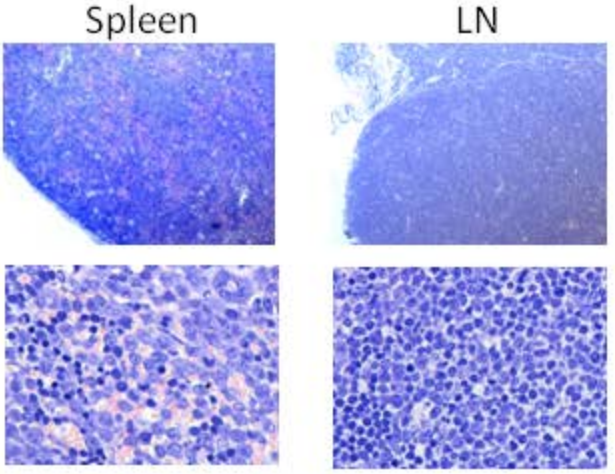

Supplementary Fig.10

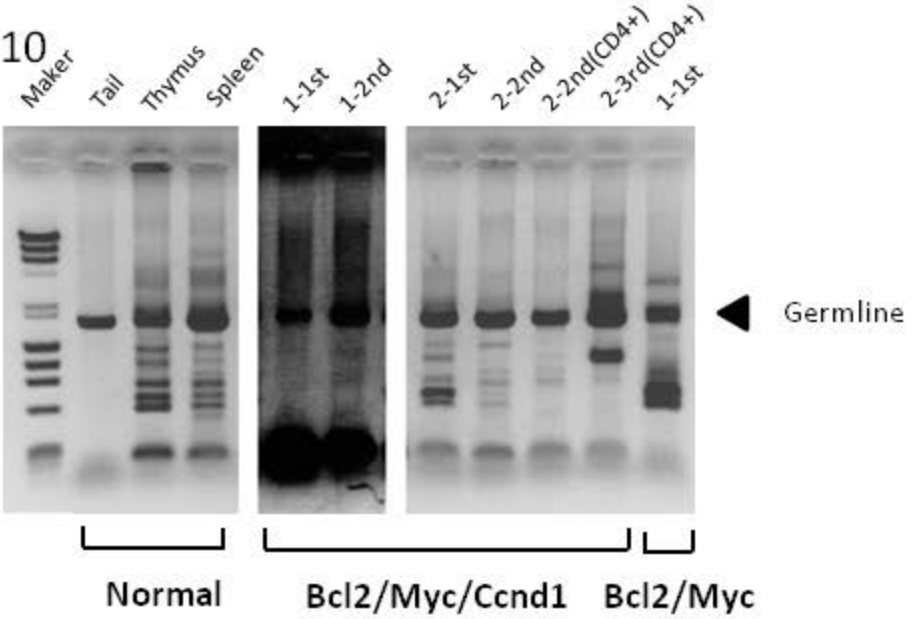

Supplementary Fig.11